

# International Conference on Space Optics—ICSO 2012

Ajaccio, Corse

9–12 October 2012

*Edited by Bruno Cugny, Errico Armandillo, and Nikos Karafolas*



## *Design of a fiber-optic interrogator module for telecommunication satellites*

*Philipp Putzer*

*Alexander W. Koch*

*Markus Plattner*

*Andreas Hurni*

*et al.*



# Design of a Fiber-Optic Interrogator Module for Telecommunication Satellites

## Radiation Test Results of Optical Components

Philipp Putzer, Prof. Alexander W. Koch

Institute of Measurement Systems and Sensor Technology  
Technische Universität München  
Munich, Germany  
p.putzer@tum.de

Markus Plattner, Andreas Hurni, Markus Manhart

Kayser-Threde GmbH  
Munich, Germany

**Abstract**— In this paper we present the results of the radiation tests performed on the optical components of the fiber-optic interrogator module as a part of the Hybrid Sensor Bus (HSB) system. The HSB-system is developed in the frame of an ESA-ARTES program and will be verified as flight demonstrator onboard the German Heinrich Hertz satellite in 2016. The HSB system is based on a modular concept which includes sensor interrogation modules based on I<sup>2</sup>C electrical and fiber Bragg grating (FBG) fiber-optical sensor elements. Onboard fiber-optic sensing allows the implementation of novel control and monitoring methods. For read-out of multiple FBG sensors, a design based on a tunable laser diode as well as a design based on a spectrometer is considered.

The expected and tested total ionizing dose (TID) applicable to the HSB system is in the range between 100 krad and 300 krad inside the satellite in the geostationary orbit over a life time of 15 years. We present radiation test results carried out on critical optical components to be used in the fiber-optic interrogation module. These components are a modulated grating Y-branch (MGY) tunable laser diode acting as light source for the tuning laser approach, the line detector of a spectrometer, photodetectors and the FBG sensors acting as sensor elements. A detailed literature inquiry of radiation effects on optical fibers and FBG sensors, is also included in the paper.

The fiber-optic interrogator module implemented in the HSB system is based on the most suitable technology, which sustains the harsh environment in the geostationary orbit.

**Index Terms**—Radiation Effects, Geostationary, Temperature Sensing, Fiber-Optics, Fiber-Bragg Gratings (FBG, Tunable Laser)

### I. INTRODUCTION

State-of-the-art telecommunication satellite platforms have to process a tremendous amount of monitoring data to fulfill tasks such as attitude and orbit control. Especially for temperature monitoring, hundreds of sensors are required. They are currently point-to-point (p2p) wired in a star configuration covering the whole satellite. This results in a complex sensor harness which increases mass, assembly, integration and test (AIT) effort and therefore the overall satellite costs. All p2p-wired temperature sensors are fed to a multiplexer to be queried by the satellite management unit

(SMU). This results in a high SMU processor load only for monitoring temperature housekeeping data. An additional problem arises due to the inflexibility of the p2p wiring. Errors in the sensor harness or later changes in the number of sensor or their positions cause a high integration effort and increases the costs dramatically.

The Implementation of an onboard sensor network wherein the individual transducers are connected via sensor buses to the HSB system significantly relieves the SMU and will directly result in a very flexible and new state-of-the-art sensor system. The HSB controller will be responsible for the sensor read out, the data evaluation and for alarm or interrupt based alert functions if a sensor is out of range.

### A. HSB System Design

In Figure 1 the basic design of the HSB system is shown. The Intelligent Power Module (IPM) contains all necessary components for the generation of the HSB secondary power, the control processor and the communication interface. The current system is designed that two different types of sensors can be read out, namely integrated electrical temperature sensors with an I<sup>2</sup>C interface and fiber-optic FBG temperature sensors. Therefore two independent modules are designed, the I<sup>2</sup>C interrogator module (IIM) for electrical temperature sensors and the fiber-optic interrogator module (FIM) for fiber-optic temperature sensors.

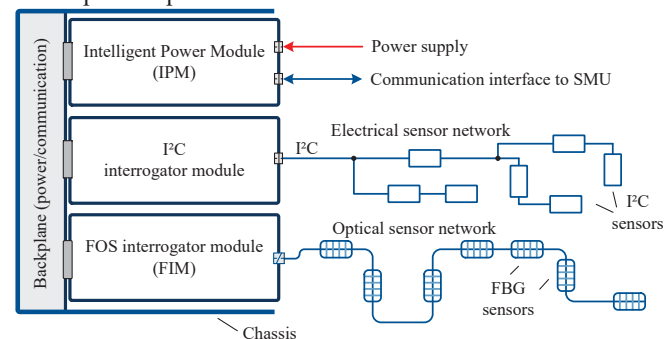


Figure 1: Concept of the HSB system with Intelligent Power Module (IPM), I<sup>2</sup>C Interrogator Module (IIM) and Fiber-Optic Interrogator Module (FIM).

Specially for the FIM fiber-optic components are necessary. Thus the main focus of the paper lies on the

radiation test results of the fiber-optical and electro-optical components.

### B. Mission Radiation Environment

The HSB system shall be implemented onboard the German technology demonstrator “Heinrich-Hertz Satellite (H2-Sat)”. This satellite is based on the Small- GEO platform from OHB-System AG. All mission specific requirements such as radiation loads, power and mass budgets and all other requirements for the contribution on the H2-Sat mission are derived from the “General Equipment Requirement Document (GERD)”. For component testing in terms of radiation tests two important parameters are to be considered, namely the total ionizing dose (TID) value and the non-ionizing energy loss (NIEL). NIEL results in degeneration due to displacement damage in the crystal lattice structure. Electronic components show a different sensitivity to TID or NIEL effects. A detailed list summarizing which type of component is sensitive to which radiation effect can be found in the ECSS-E-10-12A standard [1].

In Figure 2 the TID for silicium (Si, red curve) and the NIEL for silicium (NIEL-Si, black curve) in dependence of the alumina (Al) shielding is plotted. For the system design we assum an aluminum shielding thickness of 5 mm (including satellite housing and HSB chassis) resulting in a TID of 100 krad and a NIEL of  $2 \cdot 10^6 \text{ MeV} \cdot \text{g}(\text{Si})^{-1}$ .

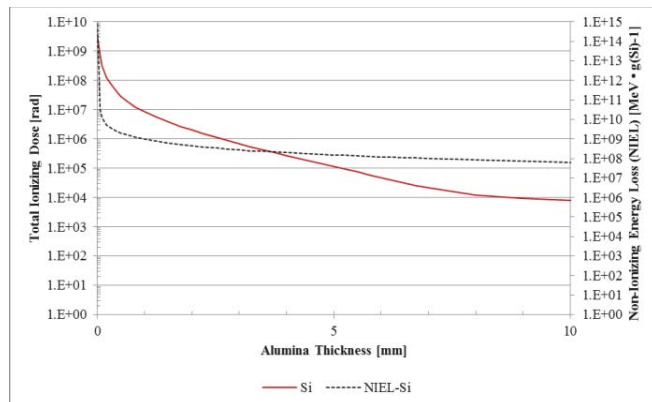


Figure 2: Total Ionizing Dose (TID) for silicium and non-ionizing energy loss (NIEL) in dependence of aluminum shielding thickness for the H2-Sat mission with a duration of 15 years in geostationary orbit [2].

## II. FIBER-OPTIC INTERROGATOR MODULE

### A. FBG Sensing – Principle

An FBG is an intrinsic optical sensor implemented directly in the core of an optical fiber. The grating is inscribed in the fiber by UV laser light [1]. The UV light compacts the glass molecules which results in a local change of the refractive index in a grating manner along the fiber. The photosensitivity of the fiber can be enhanced by increasing the germanium (Ge) concentration of the fiber core [2] or by hydrogen loading of the fiber [3] at high temperatures and high pressures.

The maximum reflectivity of an FBG is present at its Bragg wavelength  $\lambda_B$ , which is a function of the effective refractive

index  $n_{\text{eff}}$  and the grating pitch  $\Lambda$ , and can be described in approximation by the equation [5]

$$\lambda_B = 2 \cdot n_{\text{eff}} \cdot \Lambda. \quad (1)$$

If an FBG is illuminated by a broadband light source or a tunable laser light, only light corresponding to the Bragg wavelength given by equation (1) is reflected. Other parts of the wavelength spectrum can pass the FBG without be altered. Thus the FBG acts as a wavelength dependent band-stop filter. This is illustrated graphically in Figure 3.

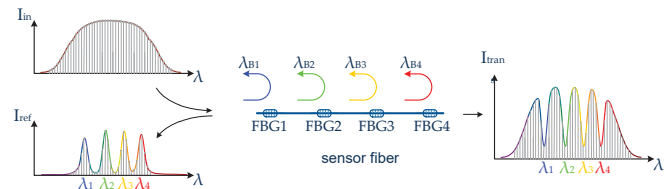


Figure 3: FBG sensor array is illuminated with a broad light source (here tunable laser) and the transmission (right side) and reflection spectra (bottom left) is shown.

By the use of this characteristic a sensor array can be implemented in a fiber. Each implemented FBG must have a different Bragg wavelength  $\lambda_B$  creating a definite assignment between the FBG sensor and the reflected spectral peak. The number of embedded FBGs is limited by the optical broadness of the illuminating light source, which is in the case of a tunable laser approximately 40 nm, and by the necessary wavelength bandwidth of each sensor.

The Bragg wavelength of an FBG is a function of the grating temperature and the mechanical strain applied to the grating. Assuming an operating wavelength of 1550 nm in the case of the HSB system, the Bragg wavelength shift (BWS)  $\Delta\lambda_B$  in dependence to the temperature change  $\Delta T$  and to the applied strain  $\Delta\epsilon$  can be calculated to [3]

$$\Delta\lambda_B = 1.209 \frac{\text{pm}}{\mu\epsilon} \cdot \Delta\epsilon + 10.338 \frac{\text{pm}}{\text{K}} \cdot \Delta T. \quad (2)$$

When evaluating the (BWS) conclusions concerning temperatures and mechanical strains can be made. However, for the HSB system the interest lies only in the evaluation of temperature changes. Changes in strain and/or vibrations are no issue here.

### B. Radiation Sensitivity of FBG Sensors

Considering the space environment wherein the system will be used, a detailed knowledge of radiation induced changes regarding the measurement accuracy is necessary. Because of the possible use of FBG sensors also in nuclear facilities many studies and tests have been carried out to observe the BWS of an FBG during and after irradiation with  $\gamma$ -rays [4].

By Grobnic et. al. it has been shown that the FBG’s written in F-doped fibers from Fujikura by the fs-IR (femto-second infrared) technology have the lowest BWS of only 3 - 7 pm after 100 kGy (10 Mrad). No change of the BWS was observed for these fibers either if the fiber was H<sub>2</sub>-loaded (type I) or not (type II). The results were identical for type I and type II FBG’s. The H<sub>2</sub> loading of FBGs in standard fibers shows a high impact on the BWS. For an unloaded SMF28 fiber a BWS

of 10 pm after 100 kGy was observed in contrast to 60 pm at the same fiber loaded with hydrogen [5]. A change of 3 - 7 pm results in a temperature deviation of 0.3 - 0.7 °C according to equation (2).

Hoeffgen et. al. pointed out that also UV written FBGs can be resistant to radiation. In the case discussed above the fs-IR written FBGs have only a 10% - 20% smaller BWS. The highest impact on the BWS has again the hydrogen loading of the fiber prior to the writing process [6]. The pressure of the hydrogen loading has only small influence which has been shown by Henschel et. al. [7]. It has also been shown that the BWS is two times higher at temperatures around -50 °C in contrast to the situation at 20 °C. This thermal annealing effect is caused by the annealing of radiation induced color centers, which change slightly the refractive index according to the temperature. In most cases the BWS shows a saturation behavior which causes after a certain dose that the overall shift remains at a constant value. If the FBGs are written in a N-doped fiber the BWS shows no saturation at doses higher than 1 MGY [8]. Therefore such fibers are absolutely not suitable for temperature monitoring in space applications.

Analysis of the BWS with different fiber coatings have been carried out by Gusarov et. al. [9]. They have shown that the stripped fiber has the lowest radiation sensitivity, whereas the ormoer coated fiber has the highest shift. This might be caused by the radiation induced aging effect in the coating which generates a mechanical stress between the fiber core and the coating.

### C. Interrogator Design

Two possible interrogator designs are considered in the HSB project. The first concept is based on a modulated grating Y-branch (MGY) tunable laser. This type of laser diode can be tuned from a wavelength of 1528 nm to 1568 nm with the help of three input currents. Inside a control FPGA a look-up table is stored wherein the relation between laser wavelengths and reflector currents is implemented. During a measurement cycle the tunable laser scans through the spectrum and the reflected light from the FBG array is measured by a photodiode. The reflected intensity signal is assigned to the output wavelength again in terms of a look-up table (LUT). Afterwards, the setup wavelength and the reflected signal are evaluated in the FPGA. The position of the reflected peak of the FBG can be estimated either by a finite impulse response (FIR) filter or a centroid algorithm. The BWS will then be evaluated by the logic implemented in the FPGA and assigned to a temperature.

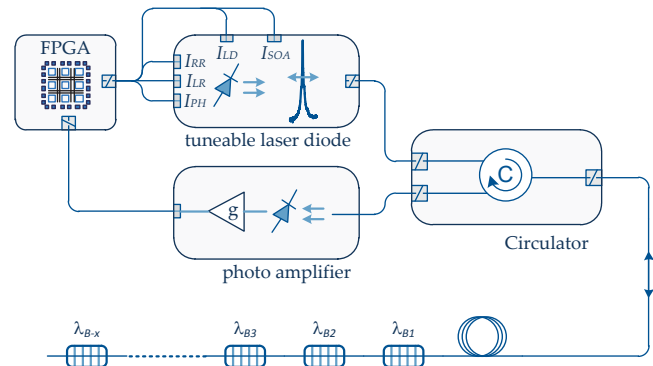


Figure 4: Fiber-optic interrogator based on a tunable laser with control FPGA, optical circulator, FBG sensors and photodiode.

The second interrogator design is based on a spectrometer and a broad-band light source, for example a superluminescent laser diode (SLD). The SLD illuminates all FBGs in the optical fiber simultaneously and the spectrometer can query all sensors nearly at the same time. Some complications arise when more than one sensor fiber shall be queried. Here the use of optical switches might be necessary. The most sensitive element in this setup is the spectrometer itself, because it is sensitive to vibrations and temperature changes and also to cosmic radiation. The design of a very stable free-space spectrometer would be the biggest challenge for this setup.

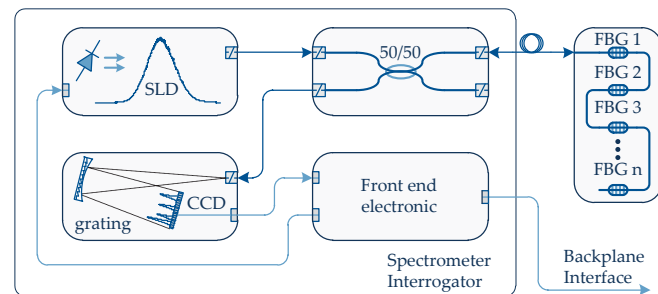


Figure 5: Fiber-optic interrogator based on a spectrometer and a broad-band light source.

### D. Tunable Laser

The tunable laser, which is the core element of the scanning laser interrogator, is a monolithic laser diode whose wavelength can be controlled electronically by three input currents. Basically two resonators are combined within the structure of this laser diode. Both resonators share the same partially light-transmissive mirror at one end. At the other end a grating structure acts as second reflector as shown in Figure 6. The MGY laser diode emits light at a wavelength where the modes of each resonator overlap. The grating structures can be modulated by carrier injection allowing a refractive index modulation of the grating material. Electric currents supplied to the grating reflectors adjust the free spectral range (FSR) of the resonators which originally is 630 GHz (5.05 nm) and 700 GHz (5.61 nm) respectively [10]. Thereby the spectra of both resonators can be shifted against each other which allows

tobring different modes of the resonators to overlap. By this so-called Vernier effect [11] wavelength tuning is achieved.

Additionally a semiconductor optical amplifier is placed behind the MGY structure to increase the output power.

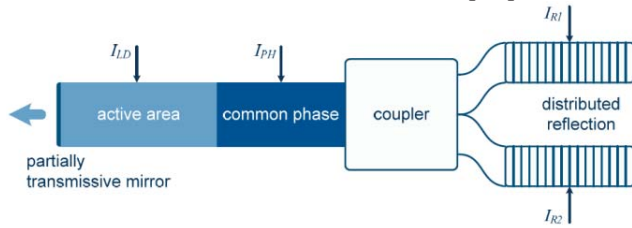


Figure 6: Principle of the MGY laser diode with left/right reflectors and common phase reflector. By carrier injection the FSR of both reflectors is changed and a tuning of the output wavelength is possible.

### III. RADIATION TEST SETUP

#### A. MGY Tunable Laser Diode

This section describes the radiation testing of the MGY laser diode. The radiation test procedure is derived from the ESCC No. 22900 [12] and adapted for the laser diode test. The TID test was carried out by the help of a Co-60 source. In a first step the LUT of the laser diode is generated and saved. This is necessary in order to identify the correct stable wavelengths of the laser and to perform a detailed analysis of the radiation induced shift of the wavelength after the test.

The following parameters are measured in-situ during the test:

- Wavelength
- Optical output power
- Reference signal and Etalon Signal
- Semiconductor Optical Amplifier and laser currents
- Reflector and phase currents

The fiber-optic interrogator module is more sensitive to changes in the output wavelength than in the output power. So a special measurement procedure has been established for the test. Every wavelength step starts at the same definite mid-wavelength  $\lambda_{mid}$ . During the whole test this wavelength can be investigated often and a long term drift over radiation exposure time can be identified. This is illustrated in more detail in Figure 7. The single wavelength points are taken from the most stable regions of the laser diode. So, no loss of wavelengths can occur during test test. In summary 37 different wavelengths plus 37 times the mid-wavelength where measured in one cycle.

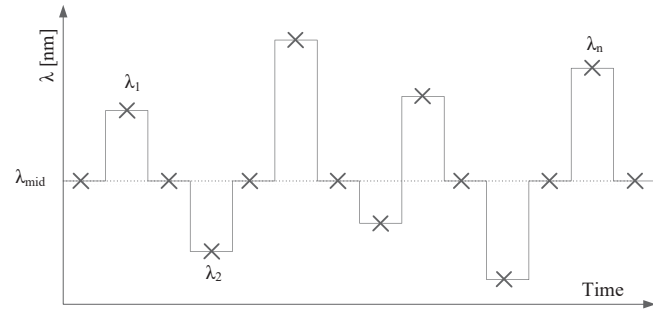


Figure 7: Measurement cycles for a scan through the lasers spectrum. Each wavelength ( $\lambda_1$  to  $\lambda_n$ ) is set up from the same mid-wavelength to identify long term drifts.

The wavelength is changed at each step according to Figure 7 until the TID of 100 krad is reached. Then the radiation exposure is stopped and the measurement is continued for at least one additional hour. Afterwards a room temperature annealing under bias is performed. All parameters are measured 12 h , 24 h and 168 h after exposure respectively. The test requires the use of a biased diode and an unbiased diode. The unbiased laser diode is measured every 10 krad TID. Thereby the on-time for the measurement is approximately 2 minutes. The laser threshold current and the slope efficiency are also measured every 10 krad by changing the laser current and monitoring the optical output power. During the test three different dose rates are applied. The duration of each step and the resulting TID is summarized in Table 1.

Table 1: Different dose rates during the Co-60 radiation test of the MGY laser diode.

Step	Dose Rate krad·h <sup>-1</sup>	Duration / ]	TID / krad
1	5	2	10
2	10	4	50
3	25	2	100

### IV. RESULTS - MGY TUNABLE LASER DIODE

In Figure 8 the results of the laser threshold and slope efficiency before radiation exposure, after 100 krad and after a 24 hour annealing phase are shown. The laser threshold is not affected by the gamma radiation. But the slope efficiency and therefore also the output power decrease from initially 6.67 mW to 6.44 mW after 100 krad. This leads to a decrease of 4.73%. After a 24 h room temperature annealing phase the optical output power reaches nearly the initial value.

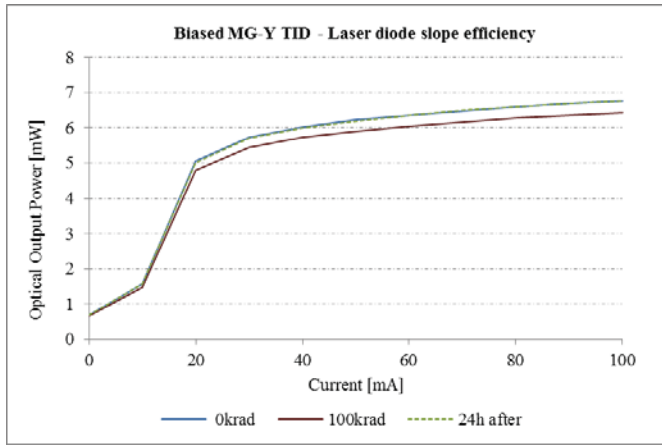


Figure 8: Optical output power of the biased MGY laser diode over TID.

The slope efficiency measurement is carried out for the biased as well as for the unbiased laser diode with different results. The unbiased laser shows a stronger decrease in the output power due to the radiation exposure. The initial value was measured to 6.44 mW, whereas the output value after 100 krad was measured to 5.84 mW. This yields to a decrement of 10.27%. In Figure 9 the output power of both diodes with respect to the radiation load is plotted. It can be seen that the output power of the unbiased diode decreases faster and reaches also a lower saturation level than the biased diode. This might be caused by thermal annealing due to current injections in the case of the biased laser. The biased laser is kept at a constant temperature of 20 °C by use of a thermoelectric cooler whereas the unbiased laser hold the ambient temperature. The electrical power consumption of the biased laser was approximately 600 mW.

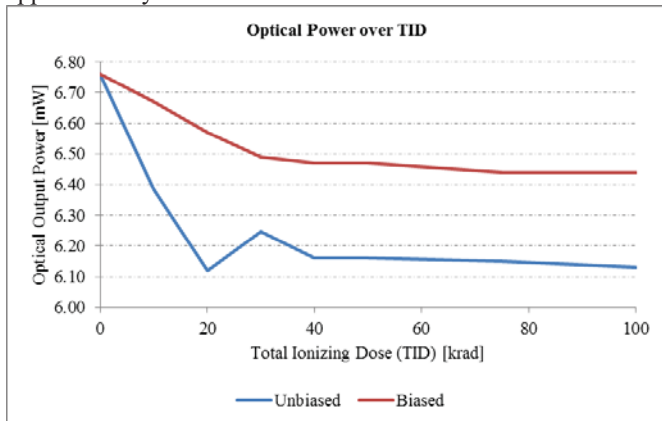


Figure 9: Optical output power for the biased (red curve) and unbiased (blue curve) laser diode respectively over TID.

A positive shift in the optical output wavelength can be observed during the gamma radiation exposure. The shift is present for all wavelengths and can be calculated by the help of the mid-wavelength to 10 pm for the biased laser diode and to 6 pm for the unbiased laser diode. In Figure 10 the deviation of single wavelengths from their original wavelength at different TID levels is shown. The maximum deviations can be identified from 6 pm to 8 pm after 100 krad.

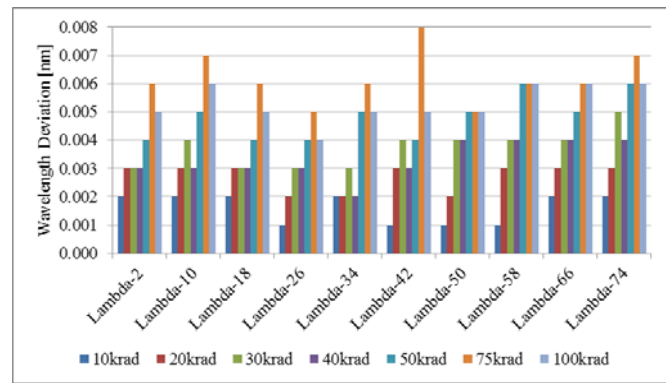


Figure 10: Wavelength deviation of different wavelengths from their original setup wavelengths at different TID levels. The maximum deviation reaches 8 pm.

## V. CONCLUSION

The tunable laser diode has shown good performance during the gamma radiation test. The wavelength shifts are in the acceptable range. Also the decrement of the output power caused by radiation is no show-stopper for the design of the fiber-optic interrogator module based on the tunable laser in the frame of the HSB system development.

## ACKNOWLEDGMENT

The development of the HSB system is funded by an ESA-ARTES 5.2 program (ESA/IPC(2009)11, 09.153.66) and supported by K. Lam, I. McKenzie and G. Furano.

The radiation tests were carried out at the Fraunhofer INT institute in collaboration with the “Nuclear Effects in Electronics and Optics” working group.

## REFERENCES

- [1] ECSS-E-10-12, "Space Engineering - Methods for the calculation of radiation received and its effects, and a policy for design margins", European Corporation for Space Standardization, ECSS Std.
- [2] General Equipment Requirements Document (GERD), v.2A, OHB-System AG.
- [3] A. D. Kersea, A. Davis, H. J. Patrick, M. LeBlanc, K. P. Koo, C. G. Askins, M. A. Putnam, and E. J. Fiebele, "Fiber grating sensors," *Journal of Lightwave Technology*, vol. 15, No. 8, p.1442, 1997.
- [4] A. F. Fernandez, B. Brichard, and F. Berghmans, "Long-term radiation effects on fiber Bragg grating temperature sensors in mixed gamma neutron fields," in RADECS, 2003.
- [5] D. Grobncic, H. Henschel, S. K. Hoeffgen, J. Kuhnenn, S. J. Mihailov, and U. Weinland, "Radiation sensitivity of Bragg gratings written with femtosecond IR lasers" *Fiber Optic Sensors and Applications VI*, vol. 7316. SPIE, 2009.
- [6] H. Henschel, S. Hoeffgen, K. Krebber, J. Kuhnenn, and U. Weinand, "Comparision of the radiation sensitivity of fiber bragg gratings made by four different manufacturer," *IEEE Transactions on Nuclear Science*, vol. 58, No. 3, p. 906, 2011.
- [7] H. Henschel, S. K. Hoeffgen, J. Kuhnenn, and U. Weinand, "Influence of manufacturing parameters and temperature on the radiation sensitivity of fiber Bragg gratings," *IEEE Transactions on Nuclear Science*, vol. 57, No.4, p. 2029, 2010.

- [8] A. I. Gusarov, F. Berghmans, A. F. Fernandez, O. Deparis, Y. Defosse, D. Starodubov, M. Decreton, P. Megret, and M. Blondel, "Behavior of fiber Bragg gratings under high total dose gamma radiation," *IEEE Transactions on Nuclear Science*, vol. 47, No. 3, p. 688, 2000.
- [9] A. I. Gusarov, C. Chojetzki, I. McKenzie, H. Thienpont, and F. Berghmans, "Effect of the fiber coating on the radiation sensitivity of type I-FBGs," *IEEE Photonics Technology Letters*, vol. 20, No. 21, p. 1802, 2008.
- [10] Syntune Widely Tunable Laser Technology, Technical Report, AB Syntune, (2005).
- [11] J. O. Westroem, "Design of a widely tunable modulated grating y-branch laser using the additive Vernier effect for improved super-mode selection," in *Proceeding of 18th IEEE International Semiconductor Laser Conference*, 2002, pp. 99–100.
- [12] ESCC Basic Specification No. 22900, "Total Dose Steady-State Irradiation Test Method", European Space Components Coordination (ESCC) Std.